Materials Sciences and Applications, 2011, 2, 435-438
doi:10.4236/msa.2011.25057 Published Online May 2011 (http://www.SciRP.org/journal/msa)

Electrochemical Behavior of Nanocrystalline $Fe_{88}Si_{12}$ Alloy in 3.5 wt% NaCl Solution

Licai Fu[1,2,*], Jun Yang[1], Qinling Bi[1], Weimin Liu[1]

[1]State Key Laboratory of Solid Lubrication, Lanzhou Institute of Chemical Physics, Chinese Academy of Sciences, Lanzhou, China;
[2]Department of Chemical and Materials Engineering, University of Alberta, Edmonton, Canada.
Email: licai1@ualberta.ca

Received February 9th, 2011; revised April 13th, 2011; accepted April 15th, 2011.

ABSTRACT

Influence of microstructure on electrochemical behavior of nanocrystalline $Fe_{88}Si_{12}$ alloy has been investigated in 3.5 *wt% NaCl solution. The results show that $Fe_{88}Si_{12}$ alloy with optimal corrosion resistance is composite of ordered Fe_3Si and disordered Fe(Si) phases and grain size of* 40 *nm. Because the ordered Fe_3Si structure is beneficial to form SiO_2 film, which possesses good corrosion resistance compared with the Fe_2O_3 film from disordered Fe(Si). Moreover, although the decreased grain size is conducive to form preservative, as the grain size decreases to* 10 *nm, the grain boundary increases to above* 30 *vol%, which is the active sites for corrosion attack.*

Keywords: *$Fe_{88}Si_{12}$ Alloy, Nanocrystalline, Microstructure, Electrochemical Behavior*

1. Introduction

Corrosion resistance is of great importance in assessing many future applications of the nanocrystalline materials. The corrosion behavior of the nanocrystalline materials has been investigated over the last two decades for a variety of materials (pure metals, alloys, and composites) [1-5]. Mishra [6] indicated that the high micro-strain in the electrodeposition Ni with grain size of 8 nm can be related to the lower corrosion rate in the 1 mol/l H_2SO_4 solution. Owing to the higher grain boundary density, the nanocrystalline Co coating exhibited good corrosion resistance comparing with coarse grained Co coating in the NaOH or NaCl solutions [7]. Xu *et al.* [8] reported that the corrosion resistance of a nanocrystalline $Ti_5Si_3C_{0.8}$ film and a nanocrystalline Ti_5Si_3 film with an average grain size of 15 nm was superior to that of Ti-6Al-4V alloy. However, Vinogradov investigated [9] that the corrosion behavior of the nanocrystalline Cu changed slightly compared with the coarse grained Cu. These researches indicate that the corrosion resistance of the nanocrystalline materials depends on their unique microstructure.

$Fe_{88}Si_{12}$ (atom ratio) alloy has been extensively investigated due to their excellent soft magnetic properties [10, 11]. However, the corrosion resistance of the $Fe_{88}Si_{12}$ alloy, especially about the nanocrystalline $Fe_{88}Si_{12}$ alloy, has not received much attention. In this paper, the electrochemical behavior of the nanocrystalline $Fe_{88}Si_{12}$ alloy has been studied by the electrochemical tests, to research influence of the grain size and phase structure on the electrochemical behavior.

2. Experimental

The different microstructures of $Fe_{88}Si_{12}$ alloys has been fabricated by a self propagating high temperature synthesis technique (SHS) [12], and annealed treat at 900˚C and 1000˚C for 1 h with air atmosphere, respectively. The grain size and phase structured of the different $Fe_{88}Si_{12}$ alloys are shown **Table 1**.

Potentiodynamic polarization curves of the different $Fe_{88}Si_{12}$ alloys were performed with 3.5 wt% NaCl solution at 25˚C. A three-electrode cell system was employed. All the results are referred to standard hydrogen electrode (SHE). The ribbons measuring 40 mm × 8 mm were cut from the samples. They were mechanically polished with 600 emery paper and rinsed with ethanol and distilled water prior to the electrochemical test. Linear polarization curves were obtained at a scan rate of 0.01 mV/s. The sample was allowed to reach a stationary open circuit potential (90 min). Then, a potential value 200 mV lower than the corrosion potential was applied for 5 minutes and the potentiodynamic scan was initiated. The specimens were examined by X-ray diffract-meter (XRD)

Copyright © 2011 SciRes.

Table 1. Grain size and phase structure of the different $Fe_{88}Si_{12}$ alloys.

Sample	Grain size	Phase structured
NC_{10}	10 nm	B2 + $D0_3$
NC_{40}	40 nm	B2 + $D0_3$
CG	>1 μm	B2

and transmission electron microscope (TEM). Specimens after the polarization tests were examined by the corrosive surfaces were characterized by a scanning electron microscope (SEM) and a PHI-5702 multifunctional X-ray photoelectron spectroscope (XPS), respectively.

3. Results and Discussion

Typical anodic potentiodynamic polarization curves of the $Fe_{88}Si_{12}$ alloys in 3.5 wt% NaCl solution are given in **Figure 1(a)**, a typical active-passive-transpassive-active behavior can be clearly observed. Normally, these passive films cover the surface of the corroded samples and increase the difficulty of Fe or Si ions migrating to surface to participate in electrochemical reaction, and thus create the passivation region where the current density is almost independent of potential.

Corrosion rate of the $Fe_{88}Si_{12}$ alloys are determined using the Stern-Geary equation from the polarization measurement [13].

$$i_{corr} = \beta_a \beta_c \Big/ \left[2.303 \times R_P \left(\beta_a + \beta_c \right) \right] \quad (1)$$

where i_{corr} is the corrosion current density, R_p the polarization resistance, β_a and β_c the anodic and cathodic tafel slopes, respectively. The R_p is determined from the slopes of the potential-current plots measured by the linear polarization curve in the range of ±10 mV about the open-circuit potential (E_{ocp}) (**Figure 1(b)**). The corrosion potential (E_{corr}) and corrosion current density (i_{corr}) are summarized in **Table 2**.

Generally, corrosion potential and corrosion current density are used to characterize the active dissolution ability of materials, while passivation current density and passivation potential are used to characterize the passivation ability of materials [14]. Corrosion potential of the NC_{40} significantly decreases and polarization resistance largely increases. Thus potentially much improve corrosion resistance comparing with NC_{10} and CG. Moreover, NC_{40} possesses lower passive current density (12.3 $\mu A \cdot cm^{-2}$) than that of NC_{10} (74.1 $\mu A \cdot cm^{-2}$) and CG (51.3 $\mu A \cdot cm^{-2}$), which indicates that the NC_{40} is easier to passivate than the NC_{10} and CG.

Figure 2 shows the SEM morphologies of the surface of the $Fe_{88}Si_{12}$ alloys after running the polarization curves. Comparing with the CG, only some slight and

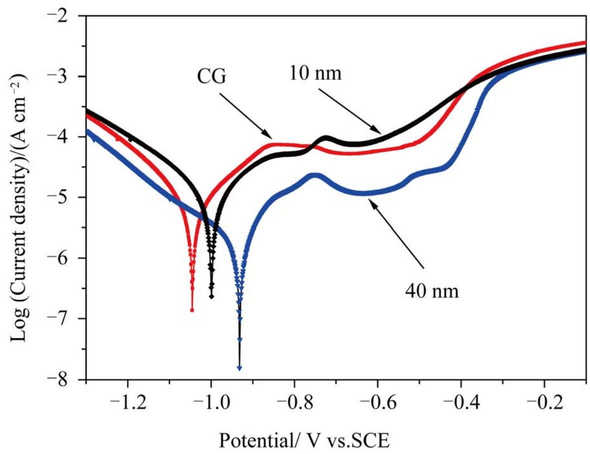

(a)

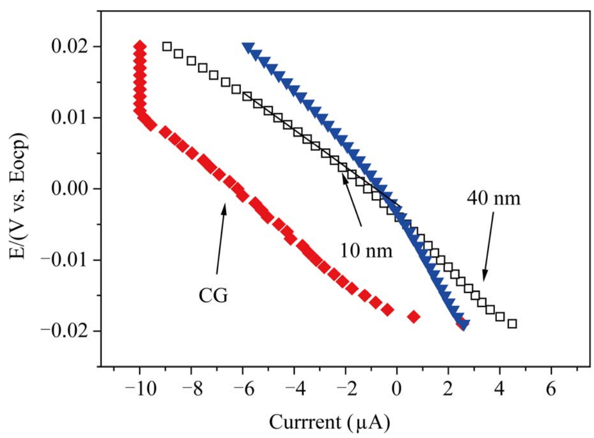

(b)

Figure 1. Potentiodynamic polarization (a) and linear polarization (b) curves of the $Fe_{88}Si_{12}$ alloys in 3.5 wt% NaCl solution.

Table 2. The fitting results of the LSV and potentiodynamic polarization tests.

Sample	E_{corr} (mV)	i_{corr} ($\mu A/cm^2$)	R_p (Ω/cm^2)	I_{pass} ($\mu A/cm^2$)
10 nm	997	70.9	3890	74.1
40 nm	932	18.2	4720	12.3
CG	1046	42.8	3500	51.3

discrete corrosion pits are observed on the surface of NC_{40} and NC_{10}. It can be associated with more protective passive film formation on NC_{40} and NC_{10} than that of CG. It is conclude that the lower corrosion rate of nanocrystalline $Fe_{88}Si_{12}$ alloys can attribute to its more protective passive film. However, some micro-crack and large corrosion hole are observed on the surface of the NC_{10} (**Figure 2(a)**), which shows the corrosion resistance decreases as the grain size decreases to 10 nm.

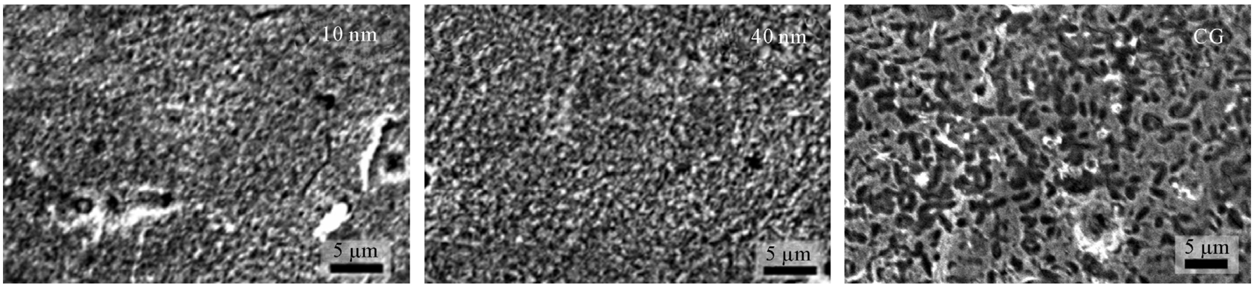

(a) (b) (c)

Figure 2. SEM morphologies of the Fe88Si15 alloys after electrochemical corrosion test.

Palumbo [15] has shown that the passivity of the 14 at% to 20 at% Si-Fe alloy, which consist of ordered Fe_3Si and few disordered Fe(Si) phases, is controlled by the formation of a silicon dioxide (SiO_2) film in 1 mol/l sulfuric acid. The research [15] indicated that the phase composition of the Fe-Si alloy influences the formation mechanisms, growth kinetics, thickness, and composition of passive layers. It also showed that high-Si content can improve the passivation behavior. Although the Si content of the Fe-Si alloy is only 12 at%, the NC_{10} and NC_{40} consist of ordered D0$_3$ Fe_3Si and disordered Fe(Si) phases. So, the SiO_2 film was observed on the surface of the NC_{10} and NC_{40} (**Figure 3**), but only Fe_2O_3 film was examined on the surface of the CG, which suggests that the corrosion resistance of the NC_{10} and NC_{40} is better than the CG.

On the other hand, with the grain size decreases to 10 nm, the grain boundaries and triple junctions increase to above 30 vol% [16], which are the active sites for corrosion attack when exposed to a corrosion environment. As a result, preferential corrosion at grain boundaries and triple junctions significantly accelerates the corrosion rate of NC_{10}. It is note that the NC_{10} possesses large numbers of micro-strain, which also makes for easier corrosion. However, the grain boundaries and triple junctions are decrease to below 5 vol% sharply as the grain size increases to 40 nm, and the micro-strain decreases as the annealing. Thus, although some ordered Fe_3Si structure transformed to the disordered Fe(Si) structure, the corrosion resistance improve as the grain size increases to 40 nm. Because the CG only composed of disordered Fe(Si) solid solution. There only Fe_2O_3 film is examined on the CG (**Figure 3**). The Fe_2O_3 film is unstable compared with the SiO_2 film [17]. So the corrosion resistance of the CG is worse than the NC_{40}.

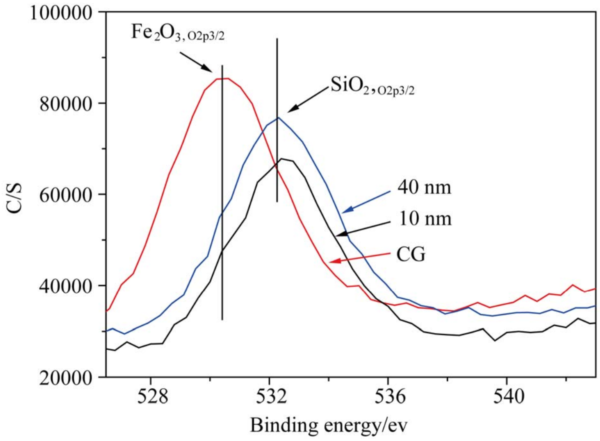

Figure 3. XPS expectra of O2p in the $Fe_{88}Si_{15}$ alloys after electrochemical corrosion test.

4. Conclusion

The electrochemical behavior of different microstructures of the $Fe_{88}Si_{12}$ alloys in 3.5% NaCl solution has been investigated. Both the $Fe_{88}Si_{12}$ alloys with grain size of 10 and 40 nm consist of ordered Fe_3Si and disorder Fe(Si) phases. But the CG is only composed of disordered Fe(Si) phase. The order Fe_3Si structure is favor to form SiO_2 film. It possesses excellent corrosion resistance comparing with the Fe_2O_3 film which forms from disordered Fe(Si). On the other hand, as the grain size decreases to 10 nm, the grain boundaries and triple boundaries increase to above 30 vol%, which are the active sites for corrosion. Based on the above two sides, the corrosion resistance of the $Fe_{88}Si_{12}$ alloy with grain size of 40 nm is optimal.

5. Acknowledgements

This work was supported by the National Natural Science Foundation of China (50801064) and the National 973 Project of China (2007CB607601)

REFERENCES

[1] S. Mato, G. Alcala, T. G. Woodcock, A. Gebert, J. Eckert and L. Schultz, "Corrosion Behaviour of a Ti-Base Nanostructure-Dendrite Composite," *Electrochimica Acta*, Vol. 50, No.12, April 2005, pp. 2461-2467. doi:10.1016/j.electacta.2004.10.071

[2] F. Renner, A. Stierle, H. Dosch, D. M. Kolb, T. L. Lee and J. Zegenhagen, "Initial Corrosion Observed on the Atomic Scale," *Nature*, Vol. 439, No. 9, February 2006, pp. 707-710. doi:10.1038/nature04465

[3] J. Balaraju, V. E. Selvi and K. Rajam, "Electrochemical Behavior of Nanocrystalline Ni-P Alloys Containing Tin and Tungsten," *Protection of Metals and Physical Chemistry of Surfaces*, Vol. 46, No. 6, 2010, pp. 686-691. doi:10.1134/S2070205110060109

[4] S. Mathur, R. Vyas, P. Kulriya, K. Asokan, K. Sachdev and S. K. Sharma, "Effects of Irradiation on the Electrochemical Behavior of the Alloy $Ti_{60}Ni_{40}$," *Journal of Alloys and Compounds*, Vol. 503, No. 1, 30 July 2010, pp. 192-193. doi:10.1016/j.jallcom.2010.04.231

[5] V. Cremaschi, I. Avram, T. Perez and H. Sirkin, "Electrochemical Studies of Amorphous, Nanocrystalline, and Crystalline FeSiB Based Alloys," *Scripta Material*, Vol. 46, No. 1, January 2002, pp. 95-100. doi:10.1016/S1359-6462(01)01204-0

[6] R. Mishra and R. Balasubramaniam, "Effect of Nanocrystalline Grain Size on the Electrochemical and Corrosion Behavior of Nickel," *Corrosion Science,* Vol. 46, No. 12, December 2004, pp. 3019-3029. doi:10.1016/j.corsci.2004.04.007

[7] L. Wang, Y. Lin, Z. Zeng, W. Liu, Q. Xue, L. Hu and J. Zhang, "Electrochemical Corrosion Behavior of Nanocrystalline Co Coatings Explained by Higher Grain Boundary Density," *Electrochimica Acta*, Vol. 52, No. 13, Mar- ch 2007, pp. 4342-4350. doi:10.1016/j.electacta.2006.12.009

[8] J. Xu, L. Liu, X. Lu and S. Jiang, "Effect of Carbon Doping on Electrochemical Behaviour of Nanocrystalline Ti_5Si_3 Film in NaCl Solution," *Electrochemistry Communications*, Vol. 13, No. 1, January 2011, pp. 102-105. doi:10.1016/j.elecom.2010.11.028

[9] A. Vinogradov, T. Mimaki and S. Hashimoto, "On the Corrosion Behaviour of Ultra-Fine Grain Copper," *Scripta Material*, Vol. 41, No. 3, July 1999, pp. 319-326. doi:10.1016/S1359-6462(99)00170-0

[10] R. Li, Q. Shen, L. Zhang and T. Zhang, "Magnetic Properties of High Silicon Iron Sheet Fabricated by Direct Powder Rolling," *Journal of Magnetism and Magnetic Materials*, Vol. 281, No. 2-3, October 2004, pp. 135-139. doi:10.1016/j.jmmm.2004.04.098

[11] M. Komatsubara, K. Sadahiro, O. Kondo, T. Takamiya and A. Honda, "Newly Developed Electrical Steel for High-Frequency Use," *Journal of Magnetism and Magnetic Materials*, Vol. 242-245, No. 1, April 2002, pp. 212-215.

[12] L. C. Fu, J. Yang, Q. L. Bi, J. Q. Ma and W. M. Liu, "Combustion Synthesis and Characterization of Bulk Nanocrystalline Fe88Si12 Alloy," *IEEE Transactions on Nanotechnology*, Vol. 9, No. 2, March 2010, pp. 218-222. doi:10.1109/TNANO.2009.2028023

[13] M. Stern and A. L. Geary, "Electrochemical Polarization," *Journal of the Electrochemical Society*, Vol. 104, No. 1, January 1957, pp. 56-63. doi:10.1149/1.2428438

[14] G. Z. Meng, Y. Li and F. H. Wang, "The Corrosion Behavior of Fe–10Cr Nanocrystalline Coating," *Electrochimica Acta*, Vol. 51, No. 20, May 2006, pp. 4277-4284. doi:10.1016/j.electacta.2005.12.015

[15] U. Wolff, F. Schneider, K. Mummert and L. Schultz, "Stability and Electrochemical Properties of Passive Layers on Fe-Si Alloys," *Corrosion*, Vol. 56, No. 12, December 2000, pp. 1195-1201. doi:10.5006/1.3280507

[16] G. Palumbo and K. T. Aust, "Structure-Dependence of Intergranular Corrosion in High Purity Nickel," *Acta Metallurgica et Materialia*, Vol. 24, No. 11, November 1990, pp. 2343-2352. doi:10.1016/0956-7151(90)90101-L

[17] A. Atkinson, "A Theoretical Analysis of the Oxidation of Fe-Si Alloys," *Corrosion Science*, Vol. 22, No. 2, February 1982, pp. 87-102. doi:10.1016/0010-938X(82)90071-3

Copyright © 2011 SciRes.